Global Change Biology

Global Change Biology (2013) **19**, 3808–3821, doi: 10.1111/gcb.12319

Characterization of an alpine tree line using airborne LiDAR data and physiological modeling

NICHOLAS C. COOPS*, FELIX MORSDORF†, MICHAEL E. SCHAEPMAN† and NIKLAUS E. ZIMMERMANN‡

Department of Forest Resource Management, University of British Columbia, 2424 Main Mall, Vancouver, British Columbia V6T 1Z4, Canada, †Remote Sensing Laboratories RSL, Department of Geography, University of Zurich – Irchel, Winterthurerstr. 190, Zurich CH-8057, Switzerland, ‡Swiss Federal Institute for Forest, Snow and Landscape Research WSL, Zürcherstrasse 111, Birmensdorf CH-8903, Switzerland

Abstract

Understanding what environmental drivers control the position of the alpine tree line is important for refining our understanding of plant stress and tree development, as well as for climate change studies. However, monitoring the location of the tree line position and potential movement is difficult due to cost and technical challenges, as well as a lack of a clear boundary. Advanced remote sensing technologies such as Light Detection and Ranging (LiDAR) offer significant potential to map short individual tree crowns within the transition zone despite the lack of predictive capacity. Process-based forest growth models offer a complementary approach by quantifying the environmental stresses trees experience at the tree line, allowing transition zones to be defined and ultimately mapped. In this study, we investigate the role remote sensing and physiological, ecosystem-based modeling can play in the delineation of the alpine tree line. To do so, we utilize airborne LiDAR data to map tree height and stand density across a series of altitudinal gradients from below to above the tree line within the Swiss National Park (SNP), Switzerland. We then utilize a simple process-based model to assess the importance of seasonal variations on four climatically related variables that impose non-linear constraints on photosynthesis. Our results indicate that all methods predict the tree line to within a 50 m altitudinal zone and indicate that aspect is not a driver of significant variations in tree line position in the region. Tree cover, rather than tree height is the main discriminator of the tree line at higher elevations. Temperatures in fall and spring are responsible for the major differences along altitudinal zones, however, changes in evaporative demand also control plant growth at lower altitudes. Our results indicate that the two methods provide complementary information on tree line location and, when combined, provide additional insights into potentially endangered forest/grassland transition zones.

Keywords: 3-PG, alpine, LiDAR, remote sensing, tree line

Received 6 March 2013 and accepted 29 June 2013

Introduction

The location of the alpine tree line is driven by a complex set of factors (Hofgaard, 1997; Moen *et al*., 2004) and a wide range of hypothesis has been published on possible driving variables. Generally, it is recognized that temperature in some form, be it average, minimum, summer or soil is the primary controller of the location of the tree line with reviews supporting this view (Körner & Paulsen, 2004; Harsch *et al*., 2009). There is recognition, however, that it is not temperature alone driving the tree line location. Körner (1998) in a detailed review of the high elevation tree line positions postulates five potentially interrelated mechanisms that may define alpine tree lines. These mechanisms include stress due to repeated damage to plant tissue by frost or the phototoxic impact of frost after the event; disturbance resulting from damage caused by wind, ice, snow amongst others; loss of reproduction, such as a reduction in pollination, seed development and dispersal; carbon balance reduction due to the uptake of carbon being insufficient to maintain growth and finally the growth limitation hypothesis, where the underlying conversion from sugars and amino acids to vegetated matter is unable to match the requirements of the species. Körner (1998) ultimately concludes it is this last hypothesis that provides the best explanation of tree line variations globally. Given that many of these underlying hypothesis are linked to climatic drivers, it is anticipated that the movement of the tree line will be responsive to changes in climate and climate warming (Kupfer & Cairns, 1996; Holtmeier & Broll, 2005) and, as a result, the upper altitudinal or

Correspondence: Nicholas C. Coops, tel. 1 604 822 6452, fax 1 604 822 9106, e-mail: nicholas.coops@ubc.ca

latitudinal tree line is an active area of investigation with the view that an improved understanding of the likely threats to alpine and arctic environments will help protect these endangered environments and their associated biodiversity (Harsch *et al*., 2009).

Despite the obvious interest in tree line position and potential movement under a changing climate, there are few monitoring programs underway worldwide. This lack of monitoring is primarily due to a lack of data, *in situ* measurements, and to some extent terminology defining the tree line itself. As stated by Körner (1998), while there is likely consensus on where the tree line actually is when viewed from an aircraft, disagreement is common when looking at the situation on the ground. These issues of data scarcity and the requirement of a synoptic view can both be addressed by remote sensing.

Remote sensing offers systematic and timely data on the tree line (Reese *et al*., 2002), however, early investigations focused on coarse spatial resolution satellite data such as NOAA AVHRR, MODIS, and SPOT VEGETATION (Olthof & Pouliot, 2010) which have spatial resolutions coarser than 250 m, and more recently ASTER and other moderate scale imagery (Heiskanen, 2006a, b) which are all unable to capture small trees, or scattered trees with large intertree distances. A more recent active remote sensing technology, known as light detection and ranging (LiDAR), is increasingly been used to measure tree and forest attributes more easily and effectively than standard forestry inventory practices (Hyyppä *et al*., 2000; Næsset, 2002; Næsset & Økland, 2002; Næsset *et al*., 2004; Coops *et al*., 2007; Wulder *et al*., 2008). LiDAR systems provide 3-D measures of the forest canopy structure using laser ranging from a known platform (aircraft) location. The location of the reflecting target is registered to a known coordinate system, and by aggregating many of these returns the dataset can be used to reconstruct individual forest stands (Persson *et al*., 2002; Morsdorf *et al*., 2004; Hilker *et al*., 2012). The use of airborne LiDAR remote sensing offers new potential to accurately delineate the tree line as it allows precise estimation of biophysical tree parameters from individual trees to large forest stands (Næsset & Nelson, 2007). Næsset & Nelson (2007) found that airborne LiDAR data acquired at a sufficiently high spatial density could be used to detect newly established trees along a tree line concluding that it would be possible to detect newly established trees over a 10-year period and thus verify if tree migration is taking place. Thieme *et al*. (2011) in a similar study found that LiDAR data acquired over two time steps were able to detect trees taller than 1 m and held promise for detecting small trees along a boreal transition tree line in Norway.

Remote sensing, however, only provides information on the current tree line and lacks any predictive capacity. This predictive capacity could be gained by integrating tree carbon dynamics modeling using process-based ecosystem models. These models are of interest as they not only predict growth but also allow users to interpret possible drivers of changes in forest growth as a result of seasonal and longer term changes in the environment (Schmid *et al*., 2006; Coops *et al*., 2011a, b). Thus, comparing the delineation of the current tree line by means of accurate remote sensing tools with model-based tree line location predictions would be beneficial to evaluate how complementary methods address some of the issues associated with tree line delineation and positioning.

In this study, we investigated the dual role remote sensing and physiological, ecosystem-based modeling can play in the delineation of the alpine tree line. To do so, we utilized airborne LiDAR remote sensing data to map tree height and density along a series of altitudinal gradients from below to above the tree line within the Swiss National Park (SNP), Switzerland. Secondly, we parameterized a simple process-based model for the dominant tree species around the tree line and ran the model using long-term climatic and terrain data. We then compared the importance of seasonal variations in four climate-driven variables that impose non-linear constraints on photosynthesis: drought, vapor pressure deficit, suboptimal temperature, and the frequency of snow and frost. When combined, these seasonal modifiers represent the total reduction in growth potential at sites across the tree line. We then compared the observed tree line using LiDAR with the physiological approaches to assess where, and under what conditions, these two approaches agreed and differed in their tree line prediction. We conclude with some proposed additional research, which could further both of these approaches for tree line detection.

Materials and methods

The Swiss National Park

The focus of this study is the eastern Ofenpass valley within the Swiss National Park (SNP), which is described in detail in Morsdorf *et al*. (2004). The area represents a dry inner-alpine valley with moderate precipitation (900–1100 mm yr^{-1}). It is surrounded by alpine peaks exceeding 3000 m above sea level (ASL). The study area is predominately covered by boreal-type forests, with spruce and mixed conifers in the lower valleys and pine-dominated stands of mountain pine (*Pinus mugo ssp. uncinata*) and stone pine (*Pinus cembra*) at medium and higher altitudes. Understory vegetation is low and dense, and principally consists of *Vaccinium* and *Ericaceae* species and of *Seslaria caerulea*. Importantly, the SNP region has regenerated

after a period of harvesting in the 18th and 19th century and has been without active management since 1914 (Morsdorf *et al.*, 2004). The location of the study area within the SNP is shown in Fig. 1.

Remote sensing of the tree line

Airborne laser scanning (ALS) data were acquired from the 11–15th September 2010 from a helicopter between 700 and 800 m above the terrain. Based on the pulse frequency, lowest sustainable flight speed and altitude, ground point sampling densities of 10 points per m^2 were achieved. Separation of ground vs. non-ground (canopy) hits was carried out using Terrascan v4.006 (Terrasolid, Helsinki, Finland), which employs iterative algorithms that combine filtering and thresholding methods (Kraus & Pfeifer, 1998; Axelsson, 1999) and classify the ALS data into either ground or non-ground returns. Secondly, a 0.5 m gridded Digital Elevation Model (DEM) was developed from all ALS ground hits. All available ground classified ALS hits were used in the DEM development on the assumption that the Terrascan classification is correct. Finally, the topographic surface was then subtracted from all non-ground ALS hits to produce estimates of vegetation height and structure.

The delineation of the tree line from ALS data, like all methods, is not well defined as there is often no definite demarcation between tree presence and tree absence, but rather a transition zone (Callaghan *et al.*, 2002; Thieme *et al.*, 2011). Trees in such areas may vary in height and spatial density due to local variations in topography, snow accumulation, cold air drainage and exposure. In this study, we utilized the definitions provided by Körner (1998) and the standards provided by the Swiss National Forest Inventory (NFI) (Brassel & Lischke, 2001), who both recognized height, cover and crown size factors when differentiating forest from non-forest. For the Swiss NFI discrimination of forest and non-forest areas is based on the width of the forested area being at least 25 m, the crown coverage greater than or equal to 20% and a dominant stand height of 3 m. With increasing width, the minimum crown coverage is allowed to decrease with the smallest acceptable threshold for the crown coverage being 20% at a minimum width of 50 m (Brassel & Lischke, 2001). In addition to using height and cover criteria, it is also possible to derive aboveground biomass from LiDAR-based observations. To do so, we utilized published equations of Lefsky *et al.* (2002) who developed a single 'simplified' regression relationship for aboveground biomass across a number of different biomes, which explained 84% of variance in aboveground biomass ($P < 0.0001$) and showed no statistically significant bias.

In order to ensure the LiDAR-derived predictions of height were accurate, we utilized field data from the long-term ecosystem monitoring site within the Swiss National Park. The field site, established in 1995, is 2 ha in size and is subject to major remeasurement every 5 years. Individual tree measurements of diameter at breast height (DBH), height and condition status are made resulting in a database of over 2450 trees (with DBH > 12 cm). Tree height is measured using a combination of actual height measurements made by a Vertex Hypsometer on a subset of the area (538 trees with DBH > 12 cm) and developing an allometric equation from DBH measurements for the remainder. To validate the LiDAR observations of tree height, 2010 only tree height measurements of the 538 measured trees were used to correlate against the LiDAR height estimates. To extract the corresponding tree locations from the LiDAR point dataset, we utilized methods of Morsdorf *et al.* (2004). First a spatial clustering routine on the LiDAR point cloud was undertaken. This produced crown segments which corresponded to individual tree crowns. Second, a geometric reconstruction of each tree was developed using a paraboloid model fitted to the tree crown to derive tree position and height.

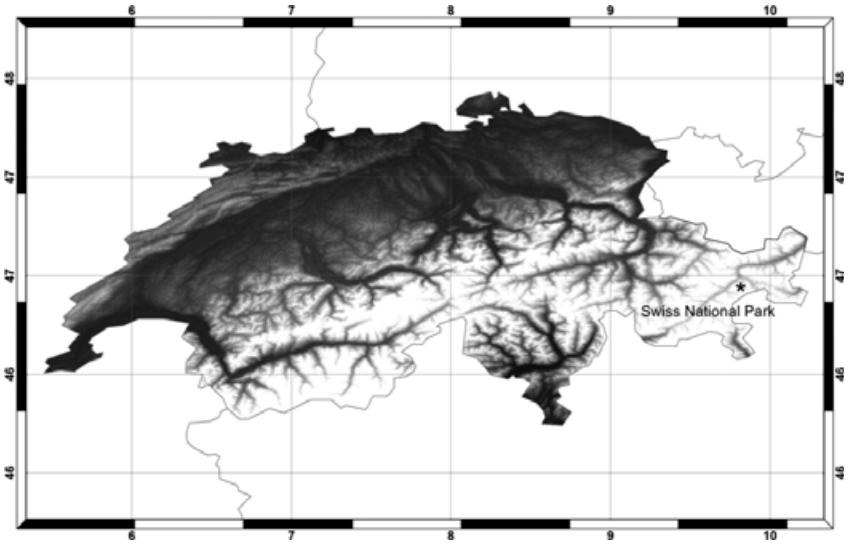

Fig. 1 Study Area Location.

Physiological modeling

The Predicting Physiological Principals of Growth (3-PG), a simple process-based model, contains a number of simplifying assumptions that have emerged from studies conducted over a wide range of forests types (Landsberg & Waring, 1997). These include the use of monthly climate data (rather than daily or annual) with little loss in the accuracy of model predictions. Each month, the most limiting climatic variable on photosynthesis is selected, based on departure from conditions that are defined as optimum (expressed as unity) or completely limited (expressed as zero) for a particular species or genotype (Coops *et al*., 2009). The ratio of actual/potential photosynthesis decreases in proportion to the reduction in the most limiting environmental factor. The fraction of production not allocated to roots is partitioned among foliage, stem and branches based on allometric relationships and knowledge of annual leaf turnover (Landsberg *et al*., 2003).

The basic model works as follows: Absorbed photosynthetically active radiation (APAR) is estimated from global solar radiation and leaf area index; and the utilized portion is calculated by reducing APAR by an amount determined by a series of modifiers that take values between 0 (system 'shutdown') and 1 (no constraint) to limit gas exchange via canopy stomatal conductance (Landsberg & Waring, 1997). The monthly modifiers include: (i) averaged day-time vapor pressure deficits (VPD); (ii) the frequency of subfreezing conditions; (iii) soil drought; and (iv) mean daily temperature. A major simplification in the 3-PG model is that it does not require detailed calculation of autotrophic respiration, assuming that it is a fixed fraction [0.47, SE $\pm$ 0.04 of gross photosynthesis (Landsberg & Waring, 1997; Law *et al*., 2000; Waring *et al*., 1998)].

Since the 3-PG model to our knowledge has not been applied to mountain pine before we utilized a published parameter set (Landsberg *et al*. (2005) derived from a similar and very closely related species, *Pinus sylvestris* (Scots pine). Scots pine is one of the most widely spread conifers in Europe, and a species which is known to coexist with mountain pine in the alpine areas of Switzerland and elsewhere. Landsberg *et al*. (2005) applied the 3-PG model to *Pinus sylvestris* in Finland and found the model provided a good description of the growth patterns of trees over long periods, including growth after repeated thinning. Landsberg *et al*. (2003) in reviewing the application of the 3-PG model to a large number of species discuss the transferability of species parameters between species and conclude that the underlying mechanisms within 3-PG represent canopy photosynthesis which does not vary between species (Valentini *et al*., 1999). Differences in radiation interception due to canopy structure can alter predictions; however, in situations of similar stand structural characteristics, these differences will also be relatively minor (Landsberg *et al*., 2003).

Given the phylogenetically and functionally close relatedness of the species to mountain pine and their coexistence in locations within our study area, we used the published parameter set, varying only site conditions to better reflect those of our study area. The parameters used in this study for the model are shown in Table 1.

Environmental data

Mean monthly minimum and maximum temperature and precipitation 100 m climate surfaces were provided by the Swiss Institute for Forest, Snow and Landscape Research generated by DAYMET (Running *et al*., 1987; Thornton *et al*., 1997; Thornton & Running, 1999) produced through interpolation of meteorological station data of MeteoSwiss (the national weather service of Switzerland). Monthly estimates of total incoming short-wave radiation were calculated using a procedure developed by Rich *et al*. (1994) and Fu & Rich (2002). The modeling approach first calculates the potential radiation at the top of the atmosphere then adjusts for slope, aspect, and elevation. Potential radiation estimates were then reduced to account for the water vapor in the air and the effects of clouds on the fraction of diffuse to direct beam incoming radiation (Running *et al*., 1987). The latter conversion takes advantage of a correlation between monthly mean temperature extremes and the transmissivity of the atmosphere (Bristow & Campbell, 1984). We set the available water holding capacity at 120 mm for a sandy loam soil throughout the region based on the previous work of Schmid *et al*. (2006). The fertility-dependent growth modifier in the 3-PG model is a function of the soil fertility rating, FR, which ranges between 0, for the poorest soils, and 1 for highly fertile soils (Landsberg & Waring, 1997). We utilized the compound topographic index (CTI) derived from the DEM as an indicator of soil processes within the study area. The CTI is based on the catenary concept (Milne, 1947), which relates soil landscape patterns on slope position and soil drainage characteristics with shallower soils tending to occur on upper slopes and crests with deeper soils occurring in convex lower slope positions (i.e. zones of aggradation). Gessler *et al*. (1995) found that CTI was significant in predicting solum depth and has been found to be a significant predictor of soil attributes such as silt percentage, organic matter content and horizon A depth (Moore *et al*., 1991). We computed the CTI from a readily available 30 m DEM for all the surrounding watersheds to provide complete coverage across the LiDAR focus area and rescaled the output between 0.4 and 0.6 with an average of 0.5.

Model runs and ALS comparison

Using the ALS-derived DEM of the study area, we stratified the landscape into 100 m elevation zones from 1800 to 2500 m, which encompassed the general tree line location. To assess the impact of aspect on the tree line, we further stratified the landscape into north and south facing slopes. Eastern and western slopes, as well as flats, were removed from the analysis. The 3-PG model was run using the long-term climate for 50 years and values of the four seasonal modifiers, leaf area index and aboveground biomass extracted within each of the elevation/aspect zones. Similarly, the ALS-derived tree height and cover was also averaged within each of the elevation/aspect zones. Finally, we compared tree heights and canopy cover per altitudinal band as derived from the two different methods.

Table 1 3-PG Parameters

3-PG Parameter	Units	*Pinus sylvestris* (Scots pine)
Biomass partitioning and turnover		
Allometric relationships & partitioning		
Foliage: stem partitioning ratio @ D = 2 cm	–	0.61
Foliage: stem partitioning ratio @ D = 20 cm	–	0.22
Constant in the stem mass vs. diam. relationship	–	0.0571
Power in the stem mass vs. diam. relationship	–	2.5698
Maximum fraction of NPP to roots	–	0.8
Minimum fraction of NPP to roots	–	0.25
Litterfall & root turnover		
Maximum litterfall rate	1 month^{-1}	0.015
Litterfall rate at t = 0	1 month^{-1}	0.01
Age at which litterfall rate has median value	Months	120
Average monthly root turnover rate	1 month^{-1}	0.015
NPP & conductance modifiers		
Temperature modifier (fT)		
Minimum temperature for growth	°C	−2
Optimum temperature for growth	°C	15
Maximum temperature for growth	°C	25
Soil water modifier (fSW)		
Moisture ratio deficit for f_q = 0.5	–	0.7
Power of moisture ratio deficit	–	9
Age modifier (fAge)		
Maximum stand age used in age modifier	Years	200
Power of relative age in function for fAge	–	4
Relative age to give fAge = 0.5	–	0.95
Stem mortality & self–thinning		
Max. stem mass per tree @ 1000 trees hectare^{-1}	kg/tree	500
Canopy structure and processes		
Specific leaf area		
Specific leaf area for mature leaves	m^2 kg^{-1}	6.0
Production and respiration		
Canopy quantum efficiency	molC/molPAR	0.05
Ratio NPP/GPP	–	0.47
Conductance		
Maximum canopy conductance	m s^{-1}	0.02
Canopy boundary layer conductance	m s^{-1}	0.2

Results

Figure 2 provides an assessment of the tree heights measured at the long-term ecosystem monitoring site within the Swiss National Park and the LIDAR tree heights. The relationship, as anticipated, is highly significant (R^2 = 0.85, P < 0.001 with an RMSE = 0.70 m). As expected, the LiDAR tree heights are consistently slightly lower than field height measurements due to fact that LiDAR hits rarely intercept the central apex of the crown. The RMSE error of 0.70 m, however, is indicative of the very high accuracy of the LiDAR-derived heights at the site. A number of outliers are obvious in the relationship. These are principally due to the clustering algorithm confusing separate tree crowns, which are likely overlapping vertically making the fitting of the paraboloid to the derived crown more problematic and producing errors in tree height.

As shown in Fig. 3, both the individual trees and the tree spacing detected from the ALS observations change through a cross-section of the valley. Trees lower in the valley are taller with greater canopy closure. In contrast, at the tree line, trees are shorter and more spaced apart. The very high ALS point density allows individual trees to be easily detected within this canopy height model.

Figure 4 shows that the maximum height of the vegetation across the altitudinal transects varies

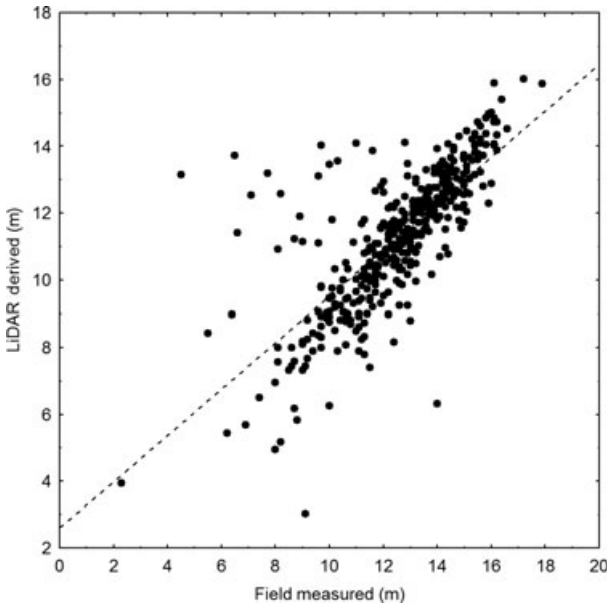

Fig. 2 Assessment of measured vs. LiDAR-derived tree heights (R^2 = 0.85, P < 0.001, RMSE = 0.70 m).

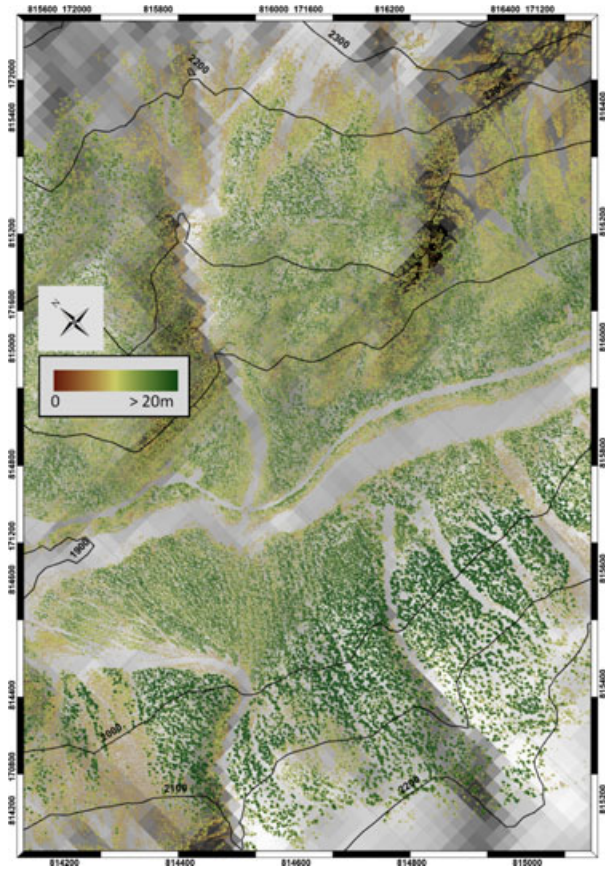

Fig. 3 LiDAR tree heights of the Ofenpass valley within the Swiss National Park (SNP). LiDAR observations are overlain the 30 m DEM of the area.

considerably from between 10 and 14 m tall at the lower altitudes through to less than 2 m at the highest altitudes. The results show that the height of the vegetation below 2200 m altitude is taller on the northern aspects than southern with, in some cases, height differences exceeding 3 m. In contrast, at altitudes above 2200 m, there is a shift with vegetation on the southern slopes being slightly taller than on the northerly aspects, although both are low at these altitudes.

The stand height criteria of a forest, defined as tree height taller than 3 m indicates that the tree line based on the LiDAR-derived heights is situated between 2200 and 2300 m and the tree line reaches higher altitudes on southern slopes compared with northern slopes. As discussed however in addition to height, the canopy cover of the trees within defined areas also provides a critical definition for forest.

Figure 5(a) shows the coverage of trees greater than 1 m, and Fig. 5(b) shows the canopy coverage of trees greater than 3 m. The results indicate that, as expected, canopy cover is greater when all trees greater than 1 m are included, ranging from 55 to 60% coverage at the lowest altitude where it is consistent until 2100–2200 m altitude. At that point, canopy cover drops quickly over the next 200 m reducing from 45–60% to 10– 30% at 2200 m. Coverage is less than 20% for both northern and southern aspects at 2200 m and above. Using the 3 m height criteria, the canopy cover is lower and more consistent among aspect. At the lowest altitude, canopy cover is between 40 and 50%. It then falls below 20% at 2200 m, the NFI minimum criterion for forest, to less than 5% at 2300 m. These results imply therefore that the cover criteria of forests are violated at lower

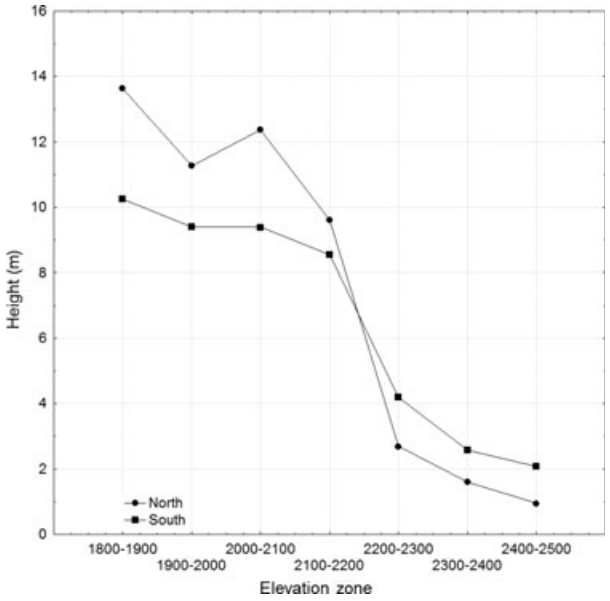

Fig. 4 LiDAR tree height by Altitudinal and Aspect Zones.

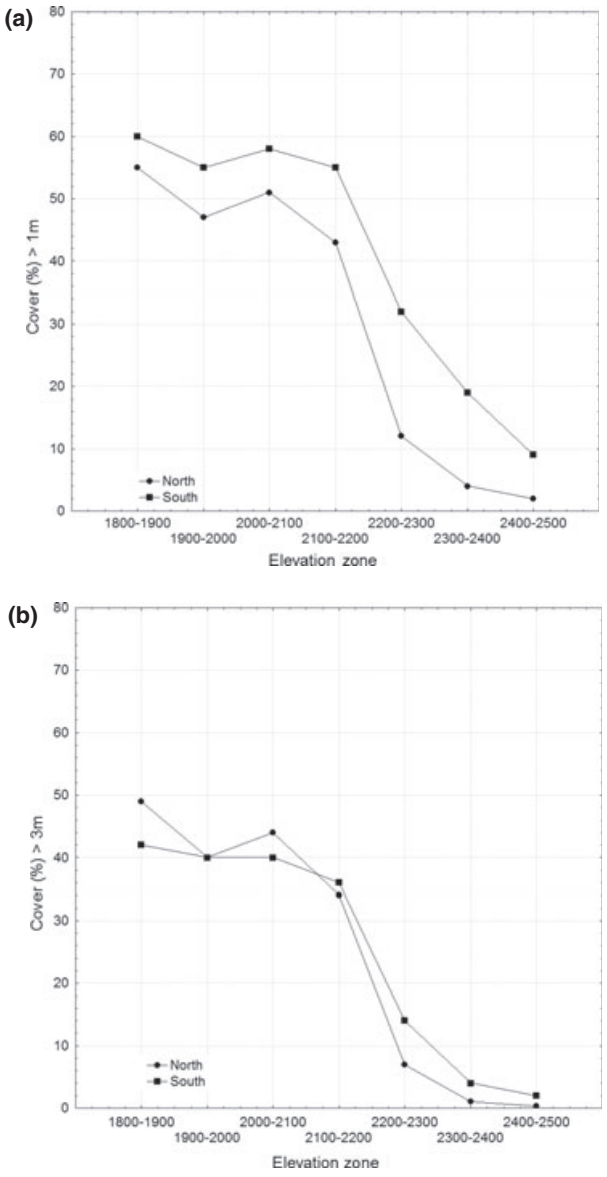

Fig. 5 Percent Canopy Cover by Altitudinal and Aspect Zones for (a) 1 m and (b) 3 m tall trees.

elevations sooner than the height criteria in this region of the SNP. Using these definitions of forest as a minimum of 20% cover and a dominant stand height of 3 m, the tree line as derived from the LiDAR data is shown in Fig. 6.

Variation in the 3-PG climatic modifiers along the north and south altitude transects, as they seasonally constrain photosynthesis on pine, is shown in Fig. 7(a–c). Optimum conditions for photosynthesis are indicated by the number 1000 (permille); whereas 0 indicates complete shutdown of the system for at least that season. Some evaporative demand VPD during the fall is evident across the elevation gradient,

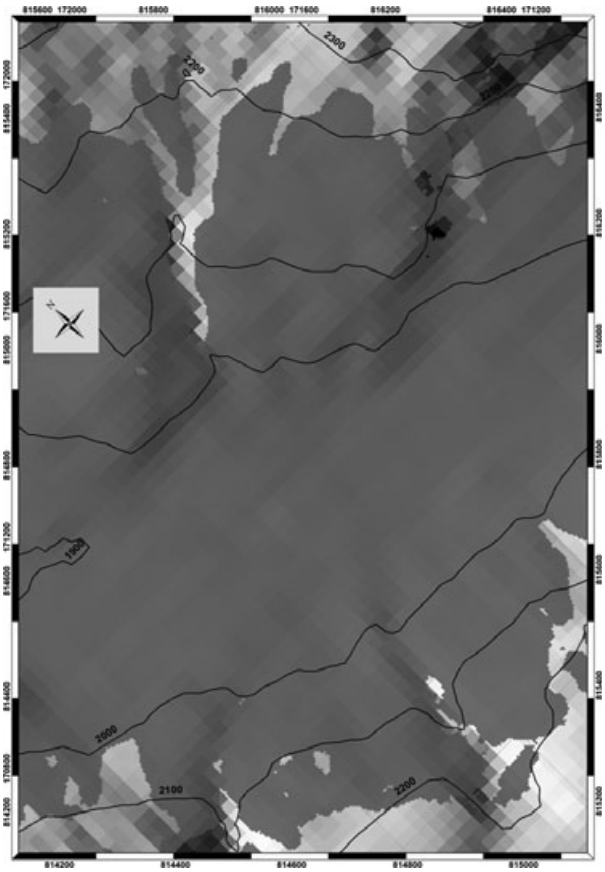

Fig. 6 Tree line as derived from the LiDAR data based on cover and height criteria.

with lower elevation sites, typically having a higher VPD stress than vegetation closer to the edge of the tree line (indicated by lower permille index numbers). Evaporative demand is highest in summer followed by spring, with less evaporative demand in fall and the lowest in winter. The mountainous areas remain sufficiently cool to reduce evaporative demand in winter to essentially zero. In all cases, both southern and northern aspects show similar stress levels along altitude transects, which may not necessarily be expected. Yet, it illustrates the fact that the input climate modifiers are interpolated from climate stations that are specifically located on flat terrain to avoid measuring such aspect differences. However, it is not clear, whether tall trees actually face significant temperature differences from variably insolated soils at the two opposing aspects, due to their marked exposure into the ambient air masses (Körner & Paulsen, 2004; Hoch & Körner, 2005).

Deviations from optimum temperature across the altitudinal gradient are shown in Fig. 7b. The results indicate that in winter, regardless of aspect, the temperature extremes are beyond the physiological limit of the

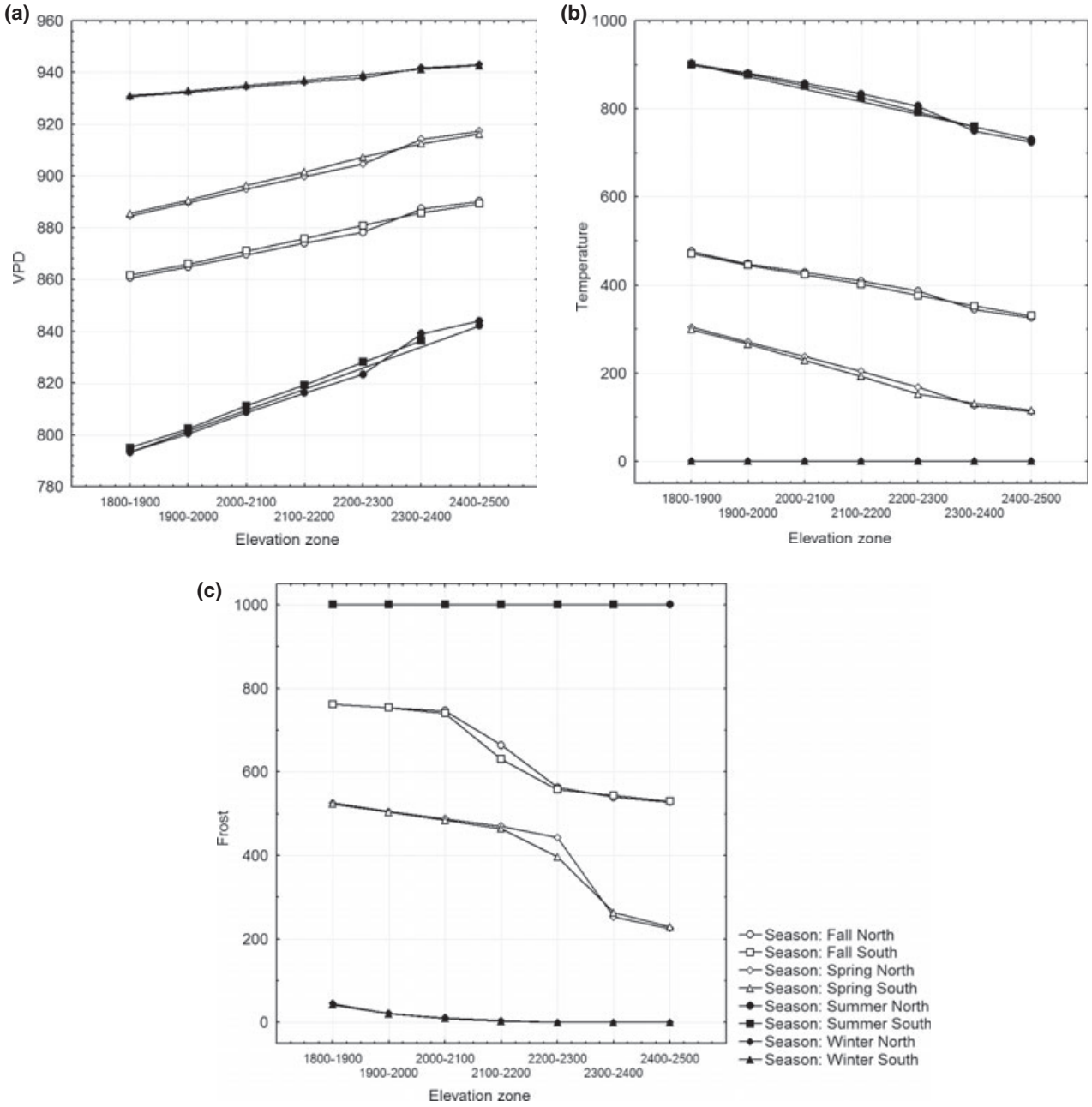

Fig. 7 3-PG Seasonal Modifiers for (a) VPD, (b) Temperature and (c) Frost by altitudinal and aspect class.

pine species, resulting in no growth and full shutdown of the vegetation. In all other seasons, the reduction in growth across the gradient is negative with higher elevation sites being constrained more by to temperature than lower ones. In summer, this relationship is the steepest, with lower altitude vegetation having only a 10% reduction in optimum growth. In contrast, vegetation at higher altitudes can have its optimum growth reduced by up to 30% due to cooler temperatures. Fall imposes less temperature stress on the vegetation than spring. The impact of frost (Fig. 7c) on the vegetation shows a markedly different response to temperature and is more indicative of the snowfall in the area. The results show that in summer there is no reduction in growth anywhere along the elevation transect. In winter, like temperature, the impact on growth is close to absolute except for a small capacity for growth at the lowest elevation range. In the spring and fall, the response is more gradual with growth reductions ranging between 20 and 50% at lower elevations and

40–80% at higher elevations. There is a clear break in the response of frost between 2011 and 2200 m elevation in fall and 2100–2300 m in spring. Similar to temperature, the stress response on the vegetation is slightly less on the northern compared with the southern slopes.

The spatial patterning of the maximum stress imposed by the climate throughout the year is shown in Fig. 8 for VPD and temperature for the Ofenpass valley within the SNP. The spatial patterns clearly show the altitudinal impact of the mountains on the north and south sides of the valley. The range of growth reduction due to VPD is relatively minor, with a small range across the altitudinal ranges. The valley floors have higher evaporative demand due to warmer temperatures and thus a reduction in photosynthetic capacity. In contrast, the temperature response is much more variable with lower constraints to growth in the valley (although still a 50% reduction over the year) to a strong limitation to growth at the higher altitudes.

The overall impact of the modifiers within the 3-PG model is to reduce the optimum quantum canopy efficiency for each month to the utilized quantum canopy efficiency. This is done through both a multiplicative and an additive approach based on the underlying stomatal response of the vegetation (Landsberg & Waring,

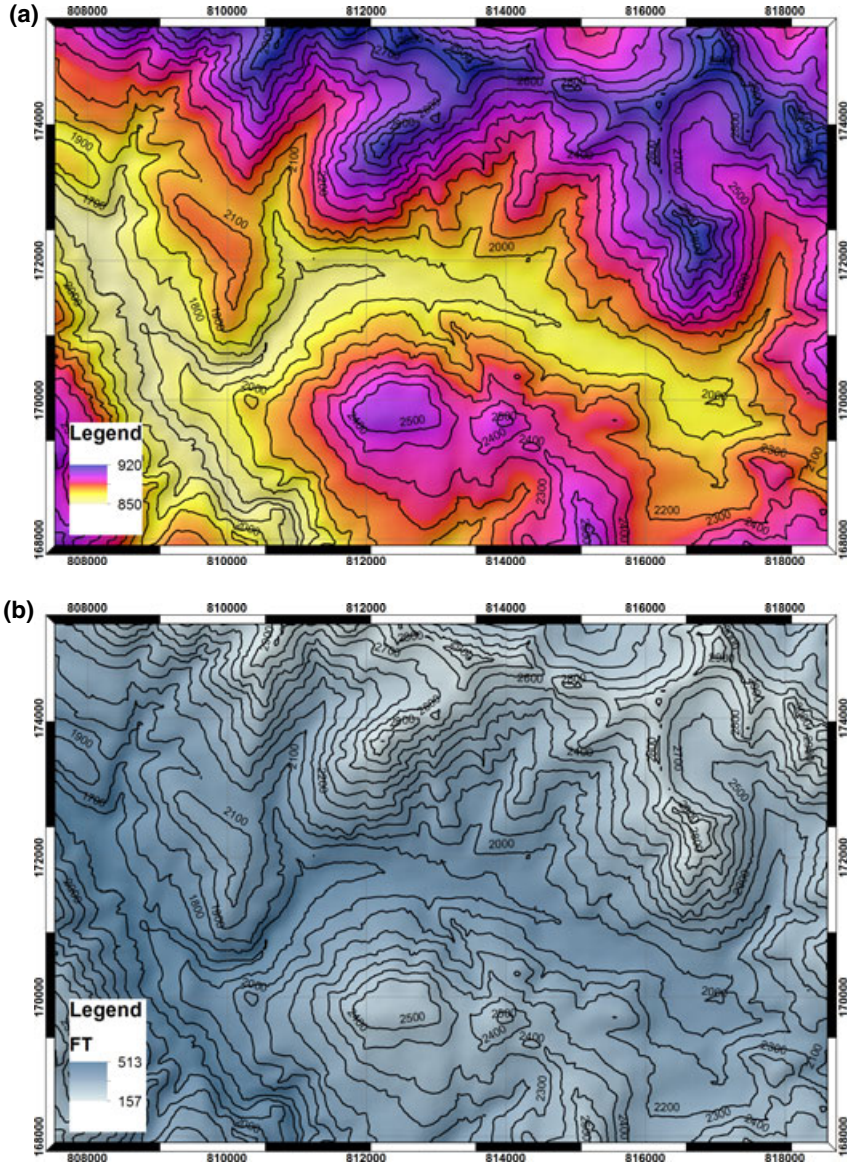

Fig. 8 Spatial Predictions of the annual minimum modifier of two 3-PG Modifiers (a) VPD and (b) Temperature for the Ofenpass valley within the Swiss National Park (SNP). Scale range from 0 (full constraint) to 1000 (no constraint to optimal photosynthesis conditions).

1997). The reduction in the optimum quantum canopy efficiency is shown as a percentage along the altitude gradient in Fig. 9 and spatially in Fig. 10. The figures clearly show that across the entire altitudinal gradient the vegetation is performing less than optimally. At the lower elevations, climate constraints throughout the year are reducing the optimum growth of the species by up to 25%. This includes the impact of temperature, frost, and VPD. In contrast, at the higher elevations the reduction is closer to 50%. At the lowest and highest points, the impact of aspect is negligible; however around the tree line, the aspect response does play a small role with an increase in the growth restriction (i.e. less growth) on the southern compared with the northern slopes. Fig. 9b provides insight into the change in the utilized quantum canopy efficiency across the transect and shows that the most abrupt change in the efficiency levels occurs around 2350 m for the northern aspects and 2250 for the southern sites. As is apparent in the figures, changes in the utilized quantum canopy efficiency are also more apparent for the northern sites than for the southern.

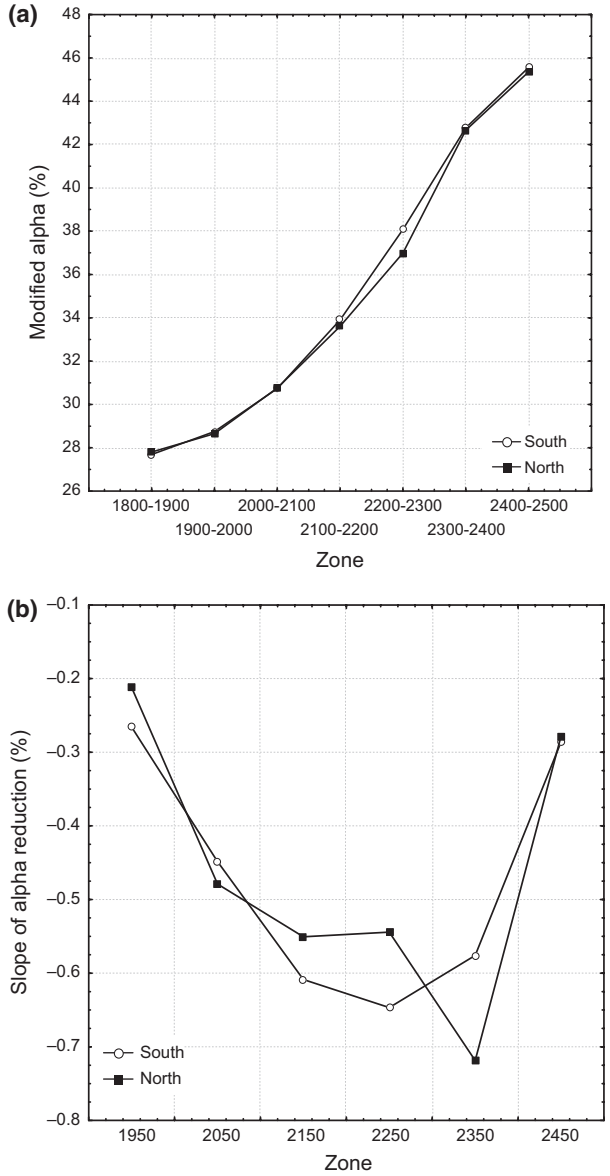

Fig. 9 (a) Reduction (in %) of the 3-PG Modeled Quantum Canopy Efficiency imposed by climatic restrictions to growth and (b) Change in slope in the 3-PG Modeled Quantum Canopy Efficiency along the altitudinal gradient.

Finally, Fig. 11a provides information on the standing aboveground biomass at each of the altitudinal/aspect zones. Schmid *et al.* (2006) provided some aboveground biomass ranges for vegetation in Switzerland and indicated that aboveground biomass (carbon) stocks of 60–90 t ha^{-1} is indicative of a closed forest, 35–60 t ha^{-1} transitioning through the tree line and less than 35 t ha^{-1} indicative of environments not supporting forest. Our 3-PG results, which show aboveground biomass as dry matter which is a factor of two greater than carbon, indicate that the threshold of 70 t ha^{-1} DM occurs in the 2200 and 2300 m altitude band for the northern aspects and slightly higher for the southern aspects which are predicted to have slightly more aboveground biomass. Finally, aboveground biomass as predicted from the LIDAR data based on the relationships of Lefsky *et al.* (2002) are shown in Fig. 11b.

Discussion

The similarity of the independent estimates of the location of the tree line indicates that both the 3-PG modeling approach and the use of LiDAR remote sensing technology can be used to offer insights into tree line location and potentially into future directional change. The aboveground biomass estimates shown in Fig. 10 follow what would be expected of this type of productive vegetated landscape and match local knowledge, which places the tree line within the region at ca. 2200 m ASL. Our results show a strong decrease in aboveground biomass along the altitudinal gradient, with the magnitude of the aboveground biomass values matching that of other studies (Schmid *et al.*, 2006), indicating that the model is suitable for predicting aboveground biomass in this conifer-dominated vegetation system.

A summary of the tree line location positions is shown in Table 2. Using a simple tree height rule of 3 m, where stands with trees greater than 3 m are defined as forest, and trees less than 3 m in height are past the tree line, the ALS data estimate the tree line occurring around 2200 m in elevation. In addition, however the NFI and others agree that a forest definition

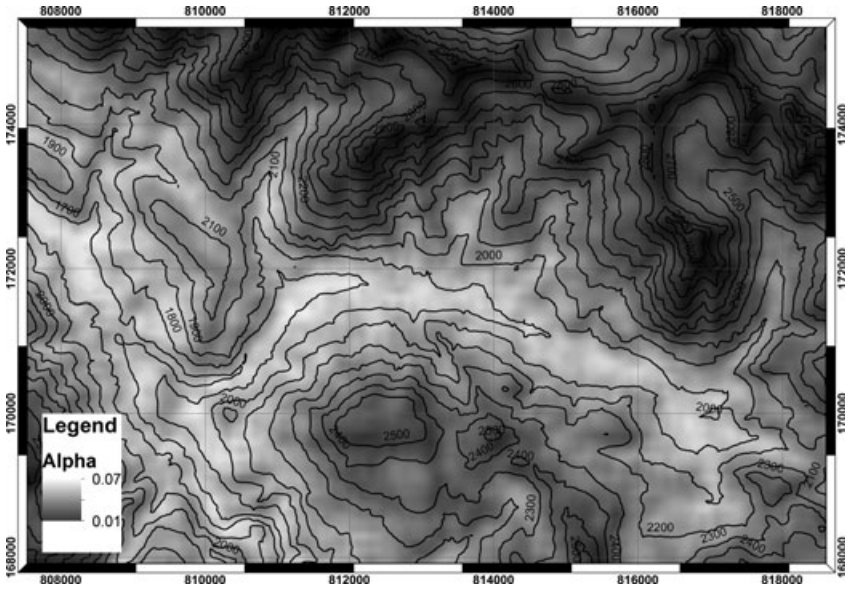

Fig. 10 Spatial Prediction of the 3-PG Modeled Quantum Canopy Efficiency with variations imposed by climatic restrictions to growth for the Ofenpass valley within the Swiss National Park (SNP).

should also include an assessment of the canopy cover in combination with the tree height. Using a definition of tree height greater than 3 m and a canopy cover of at least 20%, the position of the tree line is predicted to be lower by around 50 m in altitude. Other studies investing the size of trees at the tree line use tree height estimates lower than 3 m. Næsset & Nelson (2007) for example use a tree height threshold of 1 m. Using this broader definition of tree line tree height, the position of the tree line increases in altitude by 100–2250 m. All of these definitions thus far have utilized the ALS data acquisition. Using estimates derived from the physiological model, Schmid *et al.* (2006) define the tree line as locations with an aboveground biomass of less than 35 t ha^{-1} carbon. Our estimates indicate that using this definition with the help of the 3-PG model has the tree line slightly higher at 2250 m, similar to the 1 m tree height, 20% rule.

Like the modeling undertaken by Schmid *et al.* (2006), the 3-PG models slightly overpredict the biomass along the altitudinal gradient. Schmid *et al.* (2006) found that the Biome-BGC model predicted aboveground biomass (carbon) stocks of 60–90 t ha at 2100 m (which is similar to that of a closed forest) and 35–70 t ha^{-1} at 2300 m where the tree line should occur. As discussed, the Swiss national park historically has been subjected to a range of disturbances including a few, but likely significant stand replacing fires, in addition to harvesting in the 18th and 19th century. As a result, it is possible that the tree line is currently at a lower than naturally expected position, which is due to both anthropogenic and to a smaller extent, natural disturbances. The 3-PG model is designed to capture soil and climatic drivers on vegetation growth, but not other issues such as harvesting, fire or avalanche activity which while not currently present within the park may have historically played a role in the current tree line position. In addition, the tree line climate has been warming significantly since the mid-1960 (Gehrig-Fasel *et al.*, 2007), and the potential tree line has moved upwards between 50 m and 150 m since then (Gehrig-Fasel, 2007). It is likely that the 3-PG-derived patterns represent a slightly higher tree line, whereas the ASL-derived tree line represents the actual tree line that has been shown to respond very slowly (Gehrig-Fasel *et al.*, 2007).

The 3-PG model is designed to predict forest growth of a single species. As a result, we parameterized the model for mountain pine, one of the major pine species occurring at the tree line in this location. We have confidence therefore that the predictions of the environmental stresses, quantum canopy efficiency, and biomass are appropriate for the species below, at and above the tree line. At lower elevations in the valley, however, other species will dominate forest stands and as a result the model predictions lower in the valley are less relevant to the species that are actually occurring in those areas. Coops *et al.* (2011a, b) utilized information of forest species occurrence and multiple simulations of the model, parameterized for a number of species to overcome this limitation. If information on forest growth is desired at lower altitudes for different species, a similar approach could be applied.

For low stature alpine vegetation, Körner (1998) found that the transition of the tree line is principally

due to a reduction in the process of tissue formation rather than by a reduction in photo-assimilate itself, and found that the creation of new cells is much more sensitive to lower temperature than processes involved in photosynthesis. The 3-PG model is a light use efficiency class of model driven by photosynthesis and thus does not utilize estimates of tissue formation in its growth response. As a result, we are unable to test the hypothesis posed as a result of this review. Our results do confirm, however, that no single modifier constrains growth at the tree line. Minimum temperatures are clearly the overwhelming stress inducer at the tree line; however the impact of minimum temperature is not felt consistently either throughout the year or at different altitudinal ranges. Similarly, the frost response is also highly variable and is depended upon altitude and time of the year. Even in the winter months, the reduction in growth, while significant, does not completely shut down photosynthesis at altitudes less than 2100 m. As mentioned, soil water stress (drought) is not predicted to be a limitation to growth at all, while vapor pressure deficits will produce impacts on growth at different times of the year. Collectively, the impact on the optimum growth of the forest stands is marked, with the species having significant restrictions to growth above 2200 m elevation.

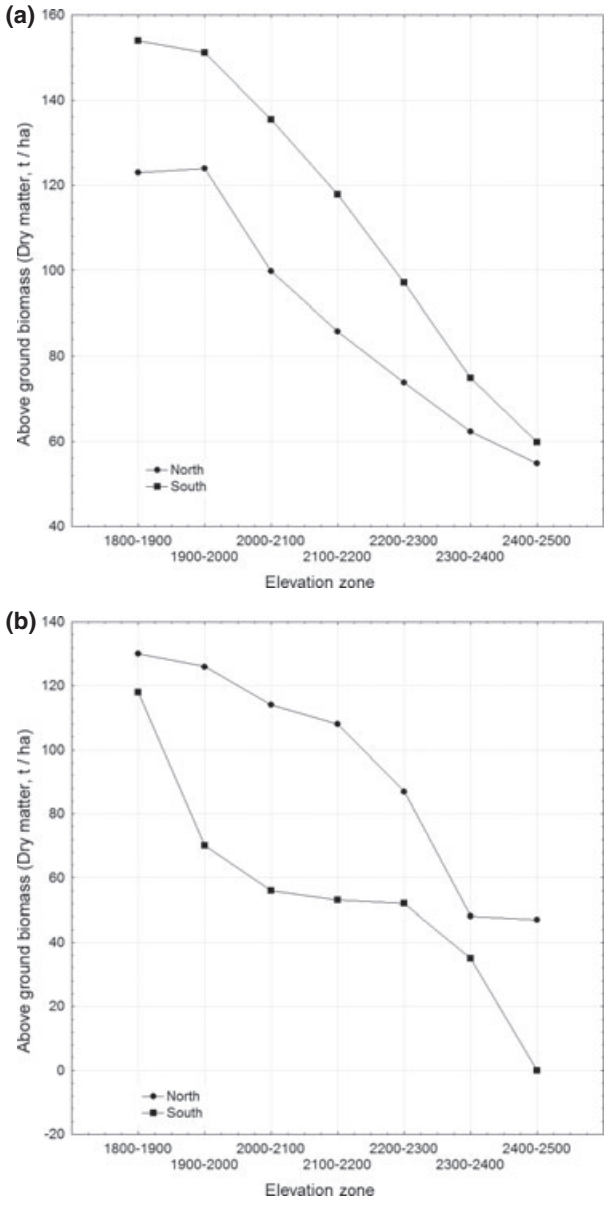

Fig. 11 (a) 3-PG Predicted AboveGround Biomass of the forest stand by Altitudinal and Aspect Zones and (b) from LiDAR.

Issues remain, however. A major simplification in 3-PG is the use of a constant factor to account for respiration of the trees, based on gross primary productivity (Nightingale *et al*., 2008). This simplification allows the model to be more easily applied across environments, but potentially can lead to errors in ecosystems where the constant allocation to respiration is not correct. It has been proposed by Schmid *et al.* (2006) for example that respiration can be underpredicted by models, which predict respiration as a function of a reference temperature. At very low temperature, this approach has shown to underestimate respiration (Schmid *et al*., 2006). While the 3-PG model does not use this reference temperature approach, it does highlight the sensitivity of these types of models to correctly account for to the respiration component when overall growth is low. However, despite the limitations of this (or any other) modeling approach, such process-driven simulations allow for prognostic analyses of tree lines under climate change, which cannot easily be done from more structural analyses as carried out by analyzing LiDAR data.

Table 2 Previously published tree line locations

Criteria	Rule	Reference	Tree line location
LiDAR height criteria	>3 m	Brassel & Lischke (2001)	2200
LiDAR cover and height criteria	>3 m and minimum 20% cover within 50 m	Brassel & Lischke (2001)	2150
LiDAR cover and height criteria	>1 m and minimum 20% cover within 50 m	Næsset & Nelson (2007)	2250
Stem mass carbon	<35t ha^{-1} carbon	Schmid *et al*., 2006	2200–2300

Acknowledgements

This research was undertaken by NCC whilst on sabbatical at University of Zurich (UZH). He acknowledges UBC Killam research fellowships and the OECD Co-operative Research Programme for fellowship awards to support his time in Switzerland. We thank Mitchell Vartanian for editorial assistance and the very helpful comments by two reviewers.

References

Axelsson PE (1999) Processing of laser scanner data - algorithms and applications. *ISPRS Journal of Photogrammetry and Remote Sensing*, **54**, 138–147.

Brassel P, Lischke H (2001) *Swiss National Forest Inventory: Methods and Models of the Second Assessment*. Swiss Federal Research Institute WSL, Birmensdorf.

Bristow KL, Campbell GS (1984) On the relationship between incoming solar radiation and daily maximum and minimum temperature. *Agricultural and Forest Meteorology*, **31**, 159–166.

Callaghan TV, Werkman BR, Crawford RMM (2002) *The Tundra-Taiga Interface and Its Dynamics: Concepts and Applications.* AMBIO, Special Report Number 12. Dynamics of the Tundra-Taiga Interface (Aug 2002), pp. 6–14.

Coops NC, Waring RH (2011) Estimating the vulnerability of fifteen tree species under changing climate in Northwest North America. *Ecological Modelling*, **222**, 2119–2129. doi:10.1016/j.ecolmodel.2011.03.033.

Coops NC, Hilker T, Wulder MA, St-Onge B, Newnham GJ, Siggins A, Trofymow JAT (2007) Estimating canopy structure of Douglas-fir forest stands from discrete-return LiDAR. *Trees-Structure and Function*, **21**, 295–310. doi:10.1007/s00468-006-0119-6.

Coops NC, Waring RH, Schroeder TA (2009) Combining a generic process-based productivity model and a statistical classification method to predict the presence and absence of tree species in the Pacific Northwest, U.S.A. *Ecological Modelling*, **220**, 1787–1796. doi:10.1016/j.ecolmodel.2009.04.029.

Coops NC, Gaulton R, Waring RH (2011a) Mapping site indices for five Pacific Northwest conifers using a physiologically based model. *Applied Vegetation Science*, **14**, 268–276. doi:10.1111/j.1654-109X.2010.01109.x.

Coops NC, Waring RH, Beier C, Roy-Jauvin R, Wang T (2011b) Modeling the occurrence of 15 coniferous tree species throughout the Pacific Northwest of North America using a hybrid approach of a generic process-based growth model and decision tree analysis. *Applied Vegetation Science*, **14**, 402–414. doi:10.1111/j.1654-109X.2011.01125.x.

Fu P, Rich PM (2002) A geometric solar radiation model with applications in agriculture and forestry. *Computers and Electronics in Agriculture*, **37**, 25–35. doi:10.1016/S0168-1699(02)00115-1.

Gehrig-Fasel J (2007) Treeline and Climate Change: Analyzing and Modeling Patterns and Shifts in the Swiss Alps. PhD Thesis, Dept. Ecology & Evolution, University of Lausanne.

Gehrig-Fasel J, Guisan A, Zimmermann NE (2007) Tree line shifts in the swiss alps: climate change or land abandonment? *Journal of Vegetation Science*, **18**, 571–582.

Gessler PE, Moore ID, McKenzie NJ, Ryan PJ (1995) Soil-landscape modelling and spatial prediction of soil attributes. *International Journal of Geographical Information Science*, **9**, 421–432.

Harsch MA, Hulme PE, McGlone MS, Duncan RP (2009) Are treelines advancing? A global meta-analysis of treeline response to climate warming. *Ecology Letters*, **12**, 1040–9. doi:10.1111/j.1461-0248.2009.01355.x.

Heiskanen J (2006a) Estimating aboveground tree biomass and leaf area index in a mountain birch forest using ASTER satellite data. *International Journal of Remote Sensing*, **27**, 1135–1158.

Heiskanen J (2006b) Tree cover and height estimation in the Fennoscandian tundra-taiga transition zone using multiangular MISR data. *Remote Sensing of Environment*, **103**, 97–114.

Hilker T, Frazer GW, Coops NC *et al.* (2012) Prediction of wood fiber attributes from LiDAR-derived forest canopy indicators. *Forest Science*, **59**, 231–242.

Hoch G, Körner C (2005) Growth, demography and carbon relations of Polylepis trees at the world's highest treeline. *Functional Ecology*, **19**, 941–951.

Hofgaard A (1997) Inter-Relationships between Treeline Position, Species Diversity, Land Use and Climate Changein the Central Scandes Mountains of Norway. *Global Ecology and Biogeography Letters*, **6**, 419–429.

Holtmeier F, Broll G (2005) Sensitivity and response of northern hemisphere altitudinal and polar treelines to environmental change at landscape and local scales. *Global Ecology and Biogeography*, **14**, 395–410. doi:10.1111/j.1466-822x.2005.00168.x.

Hyyppä H, Inkinen M, Engdahl M, Hyyppa J, Linko S, Zhu Y (2000) Accuracy comparison of various remote sensing data sources in the retrieval of forest stand attributes. *Science*, **128**, 109–120.

Körner C (1998) A re-assessment of high elevation treeline positions and their explanation. *Oecologia*, **115**, 445–459.

Körner C, Paulsen J (2004) A world-wide study of high altitude treeline temperatures. *Journal of Biogeography*, **31**, 713–732. doi:10.1111/j.1365-2699.2003.01043.x.

Kraus K, Pfeifer N (1998) Determination of terrain models in wooded areas with airborne laser scanner data. *ISPRS Journal of Photogrammetry and Remote Sensing*, **53**, 193–203.

Kupfer JA, Cairns DM (1996) The suitability of montane ecotones as indicators of global climatic change. *Progress in Physical Geography*, **20**, 253–272. doi:10.1177/030913339602000301.

Landsberg JJ, Waring RH (1997) A generalised model of forest productivity using simplified concepts of radiation-use efficiency, carbon balance and partitioning. *Forest Ecology and Management*, **95**, 209–228.

Landsberg JJ, Waring R, Coops NC (2003) Performance of the forest productivity model 3-PG applied to a wide range of forest types. *Forest Ecology and Management*, **172**, 199–214.

Landsberg J, Mäkelä A, Sievänen R, Kukkola M (2005) Analysis of biomass accumulation and stem size distributions over long periods in managed stands of Pinus sylvestris in Finland using the 3-PG model. *Tree Physiology*, **25**, 781–92.

Law BE, Waring RH, Anthoni PM, Aber JD (2000) Measurements of gross and net ecosystem productivity and water vapour exchange of a Pinus ponderosa ecosystem, and an evaluation of two generalized models. *Global Change Biology*, **6**, 155–168.

Lefsky MA, Cohen WB, Harding DJ, Parker GG, Acker SA, Gower ST (2002) Lidar remote sensing of above-ground biomass in three biomes. *Global Ecology and Biogeography*, **11**, 393–399. doi:10.1046/j.1466-822x.2002.00303.x.

Milne G (1947) A soil reconnaissance journey through parts of Tanganyika Territory December 1935 to February 1936. *The Journal of Ecology*, **35**, 192–265.

Moen J, Aune K, Edenius L, Angerbjörn A (2004) Potential effects of climate change on treeline position in the Swedish mountains. *Ecology and Society*, **9**, 16.

Moore ID, Grayson RB, Ladson AR (1991) Digital Terrain Modelling: a review of hydrological, geomorphological, and biological applications. *Hydrological processes*, **5**, 3–30.

Morsdorf F, Meier E, Kötz B, Itten KI, Dobbertin M, Allgöwer B (2004) LIDAR-based geometric reconstruction of boreal type forest stands at single tree level for forest and wildland fire management. *Remote Sensing of Environment*, **92**, 353–362.

Næsset E (2002) Predicting forest stand characteristics with airborne scanning laser using a practical two-stage procedure and field data. *Remote Sensing of Environment*, **80**, 88–99.

Næsset E, Nelson R (2007) Using airborne laser scanning to monitor tree migration in the boreal-alpine transition zone. *Remote Sensing of Environment*, **110**, 357–369.

Næsset E, Økland T (2002) Estimating tree height and tree crown properties using airborne scanning laser in a boreal nature reserve. *Remote Sensing of Environment*, **79**, 105–115.

Næsset E, Gobakken T, Holmgren J *et al.* (2004) Laser scanning of forest resources: the Nordic experience. *Scandinavian Journal of Forest Research*, **19**, 482–499. doi:10.1080/02827580410019553.

Nightingale JM, Fan W, Coops NC, Waring RH (2008) Predicting tree diversity across the United States as a function of modeled gross primary production. *Ecological Applications*, **18**, 93–103.

Olthof I, Pouliot D (2010) Treeline vegetation composition and change in Canada's western Subarctic from AVHRR and canopy reflectance modeling. *Remote Sensing of Environment*, **114**, 805–815.

Persson A, Holmgren J, Söderman U (2002) Detecting and measuring individual trees using an airborne laser scanner. *Photogrammetric Engineering and Remote Sensing*, **68**, 925–932.

Reese H, Nilsson M, Sandstro P, Olsson H (2002) Applications using estimates of forest parameters derived from satellite and forest inventory data. *Computers and Electronics in Agriculture*, **37**, 37–55.

Rich P, Dubayah R, Hetrick W, Saving S (1994) *Using Viewshed Models to Calculate Intercepted Solar Radiation: Applications in Ecology*. pp. 524–529. Available at: http://libraries.maine.edu/Spatial/gisweb/spatdb/acsm/ac94060.html (accessed 22 July 2013).

Running SA, Nemani RR, Hungerford RD (1987) Extrapolation of synoptic meteorological data in mountainous terrain and its use for simulating forest evapotranspiration and photsynthesis. *Canadian Journal of Forest Research*, **17**, 472–483.

Schmid S, Zierl B, Bugmann H (2006) Analyzing the carbon dynamics of central European forests: comparison of Biome-BGC simulations with measurements. *Regional Environmental Change*, **6**, 167–180. doi:10.1007/s10113-006-0017-x.

Thieme N, Bollandsås OM, Gobakken T, Næsset E (2011) Detection of small single trees in the forest-tundra ecotone using height values from airborne laser scanning. *Canadian Journal of Remote Sensing*, **37**, 264–274.

Thornton PE, Running SW (1999) An improved algorithm for estimating incident daily solar radiation from measurements of temperature, humidity, and precipitation. *Agricultural and Forest Meteorology*, **93**, 211–228. doi:10.1016/S0168-1923(98)00126-9.

Thornton PE, Running SW, White MA (1997) Generating surfaces of daily meteorological variables over large regions of complex terrain. *Journal of Hydrology*, **190**, 214–251.

Valentini R, Baldocchi DD, Tenhunen JD (1999) Ecological controls on land surface atmospheric interactions. In: *Integrating Hydrology, Ecosystem Dynamics and Biogeochemistry in Complex Landscapes* (eds. Tenhunen JD und Kabat P, pp. 117–145. John Wiley & Sons, West Sussex.

Waring RH, Landsberg JJ, Williams M (1998) Net primary production of forests: a constant fraction of gross primary production? *Tree Physiology*, **18**, 129–134.

Wulder MA, Bater C, Coops NC, Hilker T, White JC (2008) The role of LiDAR in sustainable forest management. *The Forestry Chronicle*, **84**, 807–826.